# Sandwich and Triple-Decker Complexes of Cobalt and Rhodium Involving the Borole Ligand: Photoelectron Spectroscopic Investigations and ab Initio CI Calculations on the Photoelectron Spectra

Isabella Hyla-Kryspin and Rolf Gleiter*

*Organisch-Chemisches Institut der Universität Heidelberg, Im Neuenheimer Feld 270, D-69120 Heidelberg, Germany*

Gerhard E. Herberich

*Anorganisch-Chemisches Institut der Technischen Hochschule, Professor-Pirlet-Strasse 1, D-52074 Aachen, Germany*

Marc Bénard*

*Laboratoire de Chimie Quantique, UPR 139 du CNRS, Université Louis Pasteur, 4 rue B. Pascal, F-67000 Strasbourg, France*

*Received June 17, 1993*®

The photoelectron (PE) spectra of four sandwich complexes involving the methylborole ligand $C_4H_4BCH_3$ are reported. Two of those molecules, namely $(\eta^5\text{-}C_4H_4BCH_3)M(C_5H_5)$ (M = Co (**1a**), Rh (**2a**), are 18-electron complexes, the other ones, namely $(\mu\text{-}\eta^5\text{-}C_4H_4BCH_3)[M(\eta^5\text{-}C_4H_4BCH_3)]_2$ (M = Co (**3a**), Rh (**4a**)), being triple-decker complexes with 30 electrons. The reported spectra are interpreted on the basis of ab initio configuration interaction (CI) calculations, carried out on model complexes where methylborole ligands have been replaced by $C_4H_4BH$ cycles (**1b–4b**), and on the basis of Green's function formalism adapted to an improved INDO procedure (**1a, 3a**). The ab initio CI calculations showed that the assignment of the two first band systems of the PE spectra is interchanged when cobalt is replaced by rhodium in isoelectronic complexes. This is a consequence of the relatively small relaxation effects and large ligand field splittings that are characteristic of the diffuse d shell of second-row transition metals. In the case of **1a** and **2a** our assignment is supported by intensity arguments from He I and He II PE spectra. The INDO results on **1a** and **3a** agree with the ab initio results.

## I. Introduction

A few years ago we studied the electronic structure of biferrocenylene and biferrocene by means of He I photoelectron spectroscopy supported by semiempirical calculations.[1] In the weakly coupled dimers the 3d ionization events can be considered as localized on one of the iron centers in a time independent manner.[1] In continuation of our investigation of metallorganic sandwich compounds containing two not directly bound metals we became interested in triple-decker complexes.[2] We have begun these studies by investigating the He I photoelectron spectra of the borole sandwich complexes $(\eta^5\text{-}C_4H_4BCH_3)M(C_5H_5)$ (M = Co (**1a**), Rh (**2a**)) and the triple-decker systems $(\mu\text{-}\eta^5\text{-}C_4H_4BCH_3)[M(\eta^5\text{-}C_4H_4BCH_3)]_2$ (M = Co (**3a**), Rh (**4a**)) which have been synthesized by Herberich et al.[3,4]

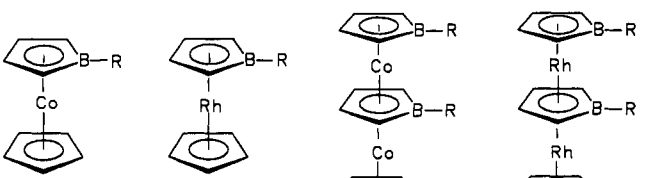


a: R= $CH_3$

b: R= H

The He II spectra are also reported for **1a** and **2a**. The photoelectron spectra are interpreted by means of semiempirical INDO (**1a, 3a**) and of ab initio MO calculations carried out at the configuration interaction (CI) level on model complexes **1b–4b**, in which the methyl substituents have been replaced by hydrogen atoms.

## II. Computational Details

All electron Hartree–Fock calculations have been carried out by means of the ASTERIX program system.[5] The Gaussian basis sets are defined as follows: for rhodium,

* Abstract published in *Advance ACS Abstracts,* April 1, 1994.

(1) Böhm, M. C.; Gleiter, R.; Delgado-Pena, F.; Cowan, D. O. *J. Chem. Phys.* **1983,** *79,* 1154.

(2) Siebert, W. *Angew. Chem.* **1985,** *97,* 924; *Angew. Chem., Int. Engl.* **1985,** *24,* 943.

(3) (a) Herberich, G. E.; Hengesbach, J.; Kölle, U.; Huttner, G.; Frank, A. *Angew. Chem.* **1976,** *88,* 450; *Angew. Chem., Int. Ed. Engl.* **1976,** *16,* 433. (b) Herberich, G. E.; Hessner, B.; Boveleth, W.; Lüthe, H.; Saive, R.; Zelenka, L. *Angew. Chem.* **1983,** *95,* 1024; *Angew. Chem., Int. Ed. Engl.* **1983,** *22,* 996; *Angew. Chem. Suppl.* **1983,** 1503. (c) Herberich, G. E.; Hengesbach, J.; Huttner, G.; Frank, A.; Schubert, U. *J. Organomet. Chem.* **1983,** *246,* 141. (d) Herberich, G. E.; Ohst, H. *Chem. Ber.* **1985,** *118,* 4303. (e) Herberich, G. E.; Boveleth, W.; Hessner, B.; Köffer, D. P. J.; Negele, M.; Saive, R. *J. Organomet. Chem.* **1986,** *308,* 153.

(4) Herberich, G. E.; Büschges, U.; Hessner, B.; Lüthe, H. *J. Organomet. Chem.* **1986,** *312,* 13. Herberich, G. E.; Hessner, B.; Saive, R. *Organomet. Chem.* **1987,** *319,* 9. Herberich, G. E.; Boveleth, W.; Hessner, B.; Hostalek, M.; Köffer, D. P. J.; Negele, M. *J. Organomet. Chem.* **1987,** *319,* 311.

0276-7333/94/2313-1795$04.50/0 

a (16,11,9) basis set taken from the (15,9,8) set optimized by Dedieu and Veillard[6] and supplemented with one s (exponent 0.310584), two p (0.217944 and 0.077527), and one d (0.071558) functions; for cobalt, a (14,9,6) basis set taken from the (13,7,5) set of Hyla-Kryspin et al.[7] and augmented with one s (0.3572), two p (0.2728 and 0.0886), and one d (0.1173) functions. The basis sets for boron and carbon are taken from Huzinaga[8] and increased with one diffuse s function, leading to (10,5) sets. Finally, the set for hydrogen is also taken from Huzinaga[9] and composed of four s-type Gaussian functions. The contractions are [7,5,5], [6,4,4], [4,3] and [2] for rhodium, cobalt, first-row atoms, and hydrogen, respectively, with all inner shells minimal.

The semiempirical INDO calculations have been carried out with an improved INDO procedure[10] which has been developed to simulate the results of high-quality ab initio calculations on organometallic systems involving first-row transition metals. This procedure cannot be applied to systems with second- or third-row transition metals, because good parametrization is not available within the INDO framework.

The geometry used for the calculations on the triple-decker complex of cobalt was adapted from the reported X-ray structure[3] for **3a**. An eclipsed conformation of the borole ligands was assumed in order to take advantage of the $C_{2v}$ (**3b**) or $C_s$ (**3a**) symmetry, even though a helical structure with average torsional angles of 66° is reported from the crystallographic data. It is well-known from previous theoretical work that the rotation barrier of cycles with the $\eta^5$ coordination mode is extremely small.[11]

No X-ray structure is available for any of the other sandwich complexes investigated in the present study. The geometrical parameters used for the calculations have then been deduced from structures available for the parent molecules.[3,4] For $(\mu\text{-}\eta^5\text{-}C_4H_4BR)[Rh(\eta^5\text{-}C_4H_4BR)]_2$, the distances from the metal to the centroids of the inner and outer borole ligands, $\Omega_{Bo}$, were assumed to be 1.85 and 1.862 Å, respectively. In the sandwich complexes $(\eta^5\text{-}C_4H_4BR)M(\eta^5C_5H_5)$ (M = Co, Rh), the distances from the metal to the centroids of the ligands were taken as Rh–$\Omega_{Bo}$ = 1.850 Å, Rh–$\Omega_{Cp}$ = 1.939 Å, Co–$\Omega_{Bo}$ = 1.645 Å, Co–$\Omega_{Cp}$ = 1.660 Å. The cycles were supposed to be planar. The geometry of the borole ligands was assumed to be similar to that of the outer ligands in the triple-decker complex of cobalt,[3] and the Cp ligand was modeled as a regular pentagon with all distances equal to 1.42 Å. The MO calculations carried out in the present work are intended to assign the photoelectron spectrum of molecules with a relatively low symmetry with either 18 or 30 electrons. The standard ΔSCF and ΔCI methods are not suited to reach this goal because of the variational collapse usually occurring for the states that are not lowest in their representation. In order to avoid such an inconvenience, it is possible to describe all states starting from a unique set of molecular orbitals and to properly account for *relaxation* by means of a multireference CI expansion *restricted to single excitation*. This method was proposed first by Doran et al.[13] and then successfully applied to several organometallic molecules and particularly to symmetric bimetallic complexes to which it is particularly well suited.[14] In our ab initio CI investigations, the starting set of MO's was a set of natural orbitals obtained from a preliminary single reference CI expansion carried out on the ground state of the neutral molecule. Furthermore, the treatment of the *correlation effects* has been fully incorporated into the method by extending to *double excitations* the multireference CI expansion designed to characterize every doublet state. The reference space has been adapted to the treatment of each state so as to maximize the weight of the reference configurations. As in the ΔCI method Davidson's correction has been introduced to smooth out the inconsistencies due to the limitations of the reference space. This method has been recently used together with ΔSCF and ΔCI calculations to interpret the photoelectron spectrum of various trioxorhenium complexes.[15]

Another very efficient way of calculating reorganization effects is a many-body perturbational approach by means of the Green's function method,[16] where relaxation and correlation effects in the ground state and the cationic states are considered. In analogy to previous studies[17] we have adopted the following approximation for the self-energy part $\Sigma(w)$ in the inverse Dyson equation.[18]

$$\Sigma(w) = \Sigma^{(2)}(w) + D4 \qquad (1)$$

This expression contains second-order terms $\Sigma^{(2)}(w)$ to approximate the self-energy part and one third-order term, $D4$.[16c]

The $j$th vertical ionization energy $I_{v,j}^{GF2}$, is related to the $j$th canonical MO energy, $\epsilon_j$, according to (2) if the inverse Dyson equation is solved via a diagonal variant. This

$$-I_{v,j}^{GF2} = \epsilon_j + \Sigma^{(2)}{}_{jj}(w_j) + (D4)_{jj} \qquad (2)$$

method was successfully applied to various metal complexes, either on the INDO[17,19] or ab initio level.[20]

(5) (a) Ernenwein, R.; Rohmer, M.-M.; Benard, M. *Comput. Phys. Commun.* **1990**, *58*, 305. (b) Rohmer, M.-M.; Demuynck, J.; Benard, M.; Wiest, R.; Bachmann, C.; Henriet, C.; Ernenwein, R. *Comput. Phys. Commun.* **1990**, *60*, 127. (c) Wiest, R.; Demuynck, J.; Benard, M.; Rohmer, M.-M.; Ernenwein, R. *Comput. Phys. Commun.* **1991**, *62*, 107.

(6) Veillard, A.; Dedieu, A. *Theor. Chim. Acta* **1984**, *65*, 215.

(7) Hyla-Kryspin, I.; Demuynck, J.; Strich, A.; Benard, M. *J. Chem. Phys.* **1981**, *75*, 3954.

(8) Huzinaga, S. Approximate Atomic Functions. Technical Report; University of Alberta: Edmonton, Alberta, Canada, 1971.

(9) Huzinaga, S. *J. Chem. Phys.* **1965**, *42*, 1293.

(10) Böhm, M. C.; Gleiter, R. *Theor. Chim. Acta* **1981**, *59*, 127, 153.

(11) (a) Albright, T. A.; Hofmann, P.; Hoffmann, R. *J. Am. Chem. Soc.* **1977**, *99*, 7546. (b) Pinhas, A. R.; Hoffmann, R. *Inorg. Chem.* **1979**, *18*, 654. (c) Chinn, J. W., Jr.; Hall, M. B. *J. Am. Chem. Soc.* **1983**, *105*, 4930.

(12) (a) Riley, P. E.; Davis, R. E. *J. Organomet. Chem.* **1976**, *113*, 157. (b) Bertani, R.; Diversi, P.; Ingrosso, G.; Lucherini, A.; Marchetti, F.; Adovasio, V.; Nardelli, M.; Pucci, S. *J. Chem. Soc., Dalton Trans.* **1988**, 2893.

(13) Doran, M.; Hillier, I. H.; Seddon, E. A.; Seddon, K. R.; Thomas, V. H.; Guest, M. F. *Chem. Phys. Lett.* **1979**, *63*, 612.

(14) (a) Granozzi, G.; Mougenot, P.; Demuynck, J.; Benard, M. *Inorg. Chem.* **1987**, *26*, 2588. (b) Quelch, G. E.; Hillier, I. H. *Chem. Phys. Lett.* **1988**, *144*, 153. (c) Clark, D. L.; Green, J. C.; Redfern, C. N.; Quelch, G. E.; Hillier, I. H. *Chem. Phys. Lett.* **1989**, *154*, 326.

(15) Wiest, R.; Leininger, T.; Jeung, G.-H.; Benard, M. *J. Phys. Chem.* **1992**, *96*, 10800.

(16) (a) Ecker, F.; Hohlneicher, G. *Theor. Chim. Acta* **1972**, *25*, 289. (b) Nerbrant, P. O. *Int. J. Quantum Chem.* **1975**, *9*, 901. (c) Cederbaum, L. S. *Theor. Chim. Acta* **1973**, *31*, 239; *J. Phys. B* **1975**, *8*, 290. (d) Cederbaum, L. S.; Domcke, W. *Adv. Chem. Phys.* **1977**, *36*, 205. (e) v. Niessen, W.; Cederbaum, L. S.; Domcke, W.; Schirmer, J. In *Computational Methods in Chemistry*; Bargon, J., Ed.; Plenum Press: New York, 1980.

(17) (a) Böhm, M. C.; Gleiter, R. *J. Comput. Chem.* **1982**, *3*, 140. (b) Böhm, M. C.; Gleiter, R.; Herberich, G. E.; Hessner, B. *J. Phys. Chem.* **1985**, *89*, 2129 and references therein. (c) Böhm, M. C.; Gleiter, R. *Chem. Phys. Lett.* **1986**, *123*, 87; *Theor. Chim. Acta* **1980**, *57*, 315.

(18) Dyson, F. *J. Phys. Rev.* **1949**, *75*, 486.

(19) (a) Gleiter, R.; Hyla-Kryspin, I.; Ziegler, M. L.; Sergeson, G.; Green, J. C.; Stahl, L.; Ernst, R. D. *Organometallics* **1989**, *8*, 298. (b) Gleiter, R.; Hyla-Kryspin, I.; Binger, P.; Regitz, M. *Organometallics* **1992**, *11*, 177.

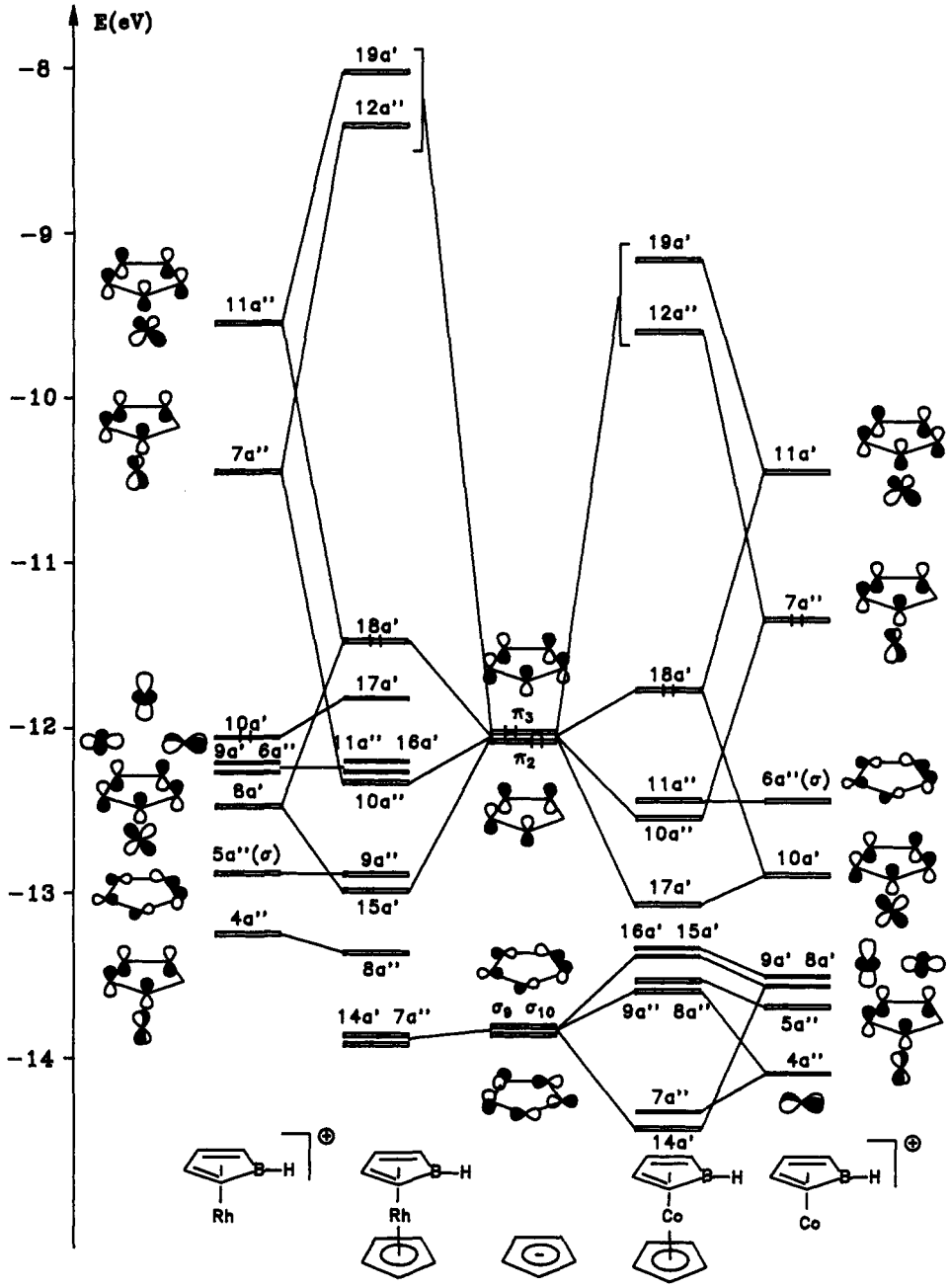


**Figure 1.** Orbital energy diagram for the sandwich complexes Cp-M-Bo (M = Co, Rh). The solid lines represent the MOs with dominant metal character.

## III. Ground State of the Neutral Molecules

A qualitative analysis of the ground state of molecules 1-4 can be obtained from orbital interaction diagrams based upon extended Hückel calculations. The frontier orbitals of the $Cp^-$ ion are well-known.[21] The HOMO, a degenerate $\pi$-orbital appearing at -12 eV, represents a donor function to the metal fragments (Figure 1). At -14 eV, degenerate $\sigma$-orbitals give weak 4-electron interactions with appropriate metal orbitals. The lowest $\pi$-orbital, very stable (-14.45 eV) and completely symmetric, is stabilized by the high-lying metal orbitals with s and $p_z$ character (not shown in Figure 1). The HOMO, a doubly degenerate combination of $\pi$-orbitals at -12 eV, is fully occupied with 4 electrons in the monoanion $Cp^-$. In the borole ring, the presence of the boron atom splits the degeneracy of those frontier orbitals that now appear as two distinct levels, $\pi_2$ and $\pi_3$, separated by 1.3 eV (-10.8 and -12.1 eV: see Figure 2). The neutral borole molecule has only 4 $\pi$ electrons including those of the fully symmetric orbital (-14.1 eV), so that the third $\pi$ orbital at -10.8 eV becomes the LUMO, or the HOMO of the dianion (Figure 2).

In spite of this energy splitting of the frontier $\pi$-orbitals, the borole dianion is isolobal with the $Cp^-$ ligand and the interactions with the metal d orbitals are qualitatively similar. More specifically, the $\pi_3$-orbital of borole with $b_2$ symmetry (the LUMO of the neutral borole) is strongly stabilized by an interaction with the metal $d_{yz}$ orbital and becomes part of the occupied set of the $[M-Bo]^+$ fragment (Figure 1). In a purely ionic picture of the bonding, the borole ligand should then be formally considered as a dianion and the metal assumed to be in oxidation state III. A covalent interpretation of the bonding, involving neutral metal and ligand fragments and a strong back-

(20) Taylor, D. A.; Hillier, I. H.; Vincent, M.; Guest, M. F.; MacDowell, A. A.; v. Niessen, W.; Urch, D. S. *Chem. Phys. Lett.* **1985**, *121*, 482.

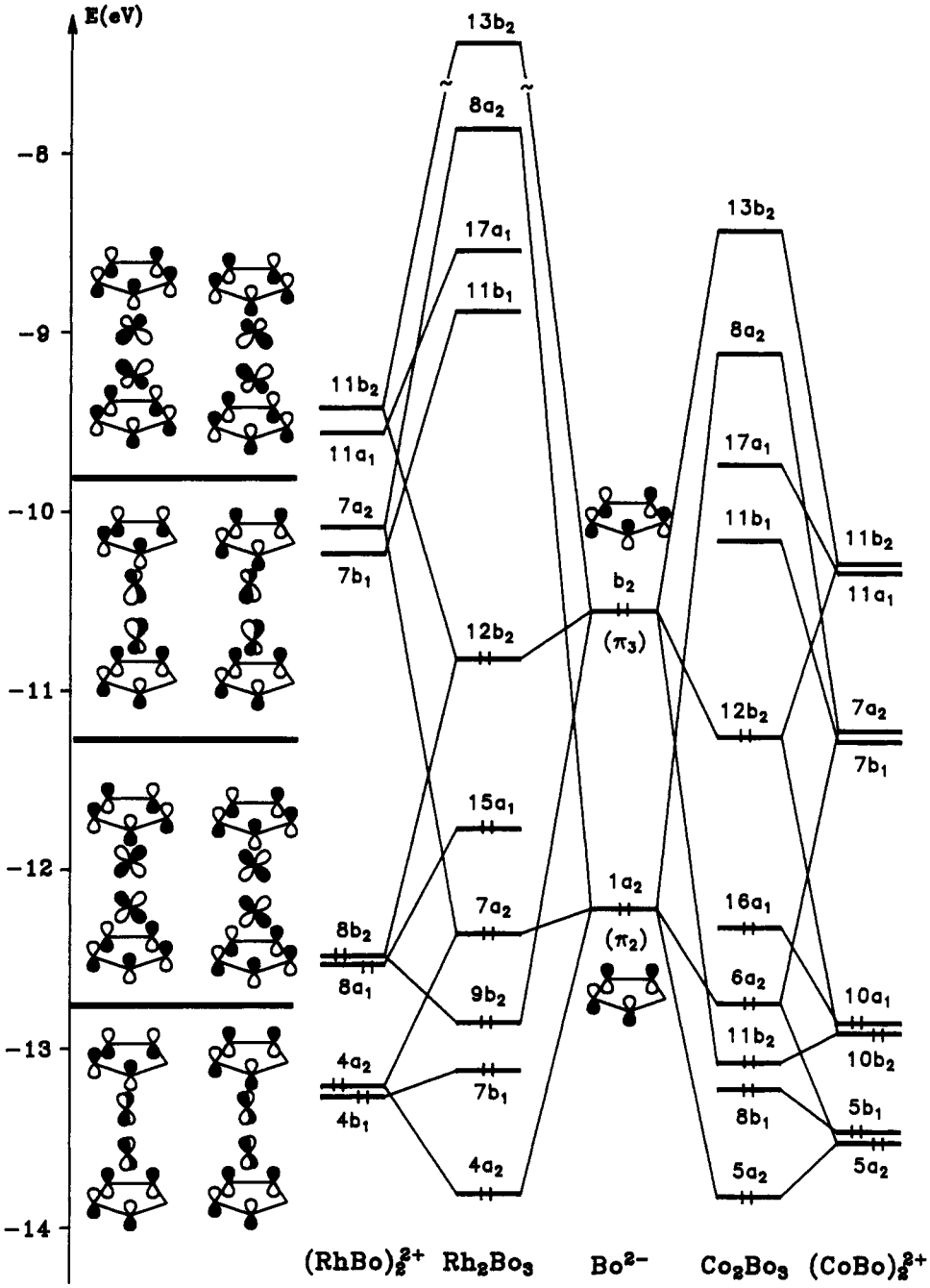


**Figure 2.** Orbital energy diagram for the frontier orbitals of Bo–M–Bo–M–Bo (M = Co, Rh) with main $\pi$-ligand character.

bonding interaction from the metal to the borole $\pi_3$ level, also represents quite a convenient scheme, particularly suited to interpret the strong metal–ligand interactions occurring in the sandwich complexes of rhodium. It is only to avoid too much complexity that the metal atoms will be considered as $d^6$ species in complexes **1–4**, which makes them isolobal to ferrocene, ruthenocene, and triple-decker complexes of Fe and Ru with standard Cp ligands, respectively. The interaction diagrams leading to Cp–Co–Bo and Cp–Rh–Bo are displayed in Figure 1. The occupied orbitals 18a′ and 10a″ of the sandwich molecules can be easily correlated with the degenerate set with $e_{1g}$ symmetry obtained in the orbital diagram of metallocenes.[21,22] The underlying orbital set of metallocenes, also degenerate with $e_{1u}$ symmetry, is found to correlate with orbitals 17a′/8a″ in Cp–Co–Bo and with levels 15a′/8a″ in Cp–Rh–Bo. The three "$t_{2g}$-like" metal orbitals are relatively low-lying in the cobalt complex (7a″, below −14 eV; 15a′ and 16a′, below −13 eV). At variance with that, the metal levels in the rhodium complex, 11a″, 16a′, and 17a′, are clustered around −12 eV, just below the delocalized HOMO 18a′. Apart from this difference in the energy of the metal levels, it is clear from the diagrams of Figure 1 that the interactions between the metal and the ligand $\pi$-orbitals are much more effective in the rhodium complex, leading to a more delocalized description of the HOMO

(21) Albright, T. A.; Burdett, J. K.; Whangbo, M. H. *Orbital Interactions in Chemistry*; Wiley-Interscience: New York, 1985; Chapter 20.

(22) Van Dam, H.; Oskam, A. UV Photoelectron Spectroscopy of Transition Metal Complexes. In *Transition Metal Chemistry*; Melson, G. A., Figgis, B. N., Eds.; Marcel Dekker, Inc.: New York, 1985; Vol. 9, pp 125–308.

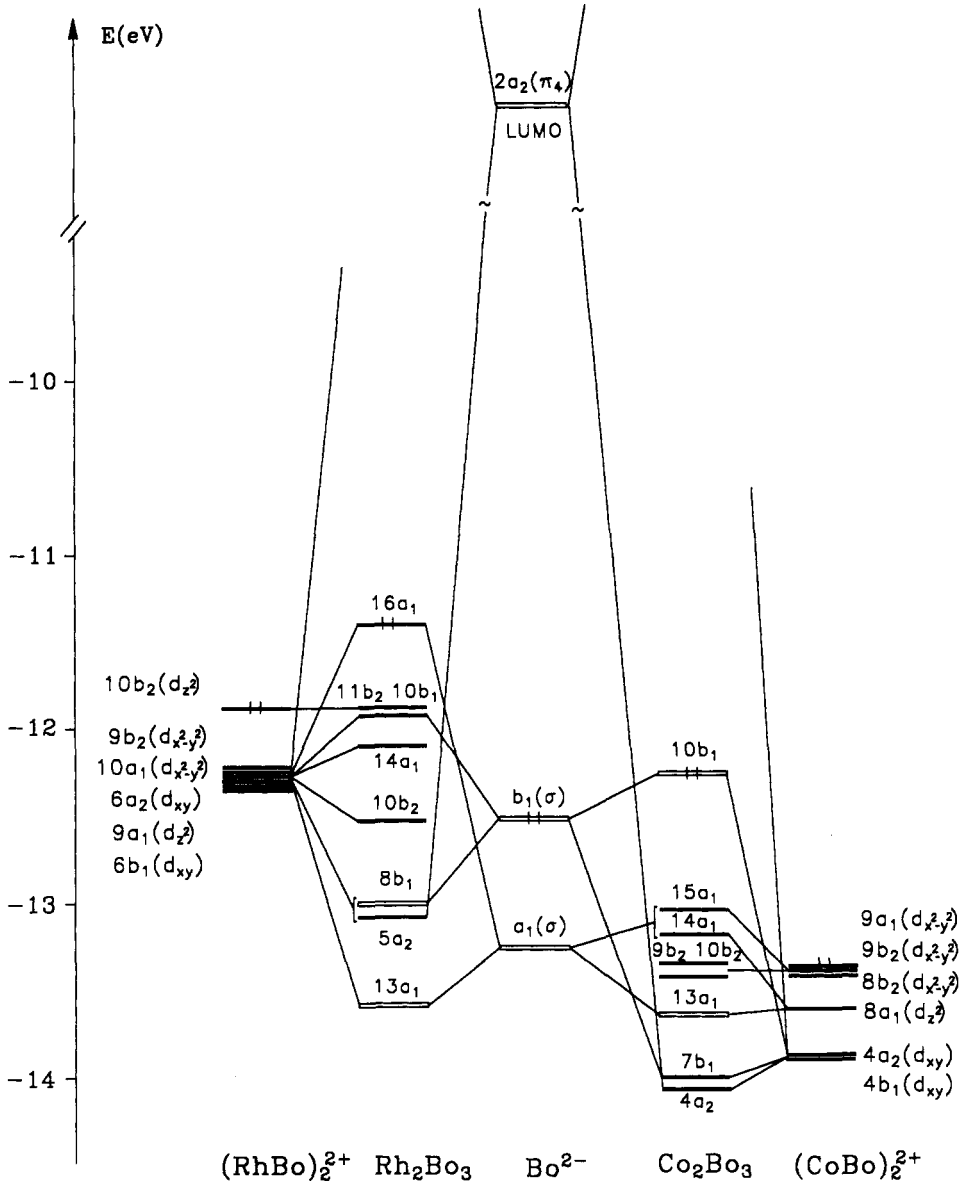


**Figure 3.** Orbital energy diagram for the frontier orbitals of Bo–M–Bo–M–Bo (M = Co, Rh) with metal and $\sigma$-ligand character. The solid lines represent the MOs with main metal character.

18a′ and of the three other stabilized orbitals with major ligand character: 10a″, 15a′, and 8a″.

Figure 2 and 3 display equivalent interaction diagrams for the triple-decker, 30-electron complexes **3** and **4**. Figure 2 displays the splitting of the frontier orbitals resulting from the interaction between $d_{xz}$ and $d_{yz}$ metal orbitals on the one hand and the $\pi$ levels of the borole ligands on the other hand. Figure 3 displays the scattering of the metal orbitals in the same complexes. Those diagrams should be compared with the standard interaction schemes obtained for Cp–M–Cp–M–Cp sandwich complexes in $D_{5h}$ symmetry,[21] accounting for the removal of the orbital degeneracy induced by the borole ligands. As a consequence, the three degenerate pairs of $\pi$-orbital combinations obtained in the $D_{5h}$ molecules correlate with the following orbital pairs in the borole complexes: $e''_1 \rightarrow (12b_2, 6a_2)$, with M = Co, $(12b_2, 7a_2)$, with M = Rh; $e'_1 \rightarrow (16a_1, 8b_1)_{Co}$ and $(15a_1, 7b_1)_{Rh}$; $e''_1 \rightarrow (11b_2, 5a_2)_{Co}$ and $(9b_2, 4a_2)_{Rh}$. Once again, the splitting of the metal levels appears more important for rhodium than for cobalt (Figure 3).

## IV. Photoelectron Spectra and Assignment

The He I and He II photoelectron spectra of **1a** and **2a** are displayed in Figure 4. The relations of the band intensities in the He I and He II spectra of **1a** and **2a** are summarized in Table 1. The He I spectra of **3a** and **4a** are shown in Figure 6. Tables 2 and 4 provide information concerning the computed ionization energies at the ab initio CI level (state, Koopmans' energy, effect of relaxation and correlation, computed ionization energy, population analysis of the natural orbital that accommodates the unpaired electron, assignment in terms of fragment orbitals, and reference to the orbital diagram of Figures 1–3). Table 3 provides information concerning the computed ionization energies of **1a** and **3a** at the semiempirical INDO level. Figures 5 and 7 present the proposed mapping between the computed ionization energies and the reported bands of Figures 4 and 6.

**IV.1. CP–Borole Sandwich Complexes.** As for the parent cyclopentadienyl sandwich complexes[22,23] the He I spectra obtained for **1a** and **2a** show a broad band centered around 13 eV that should be assigned to the

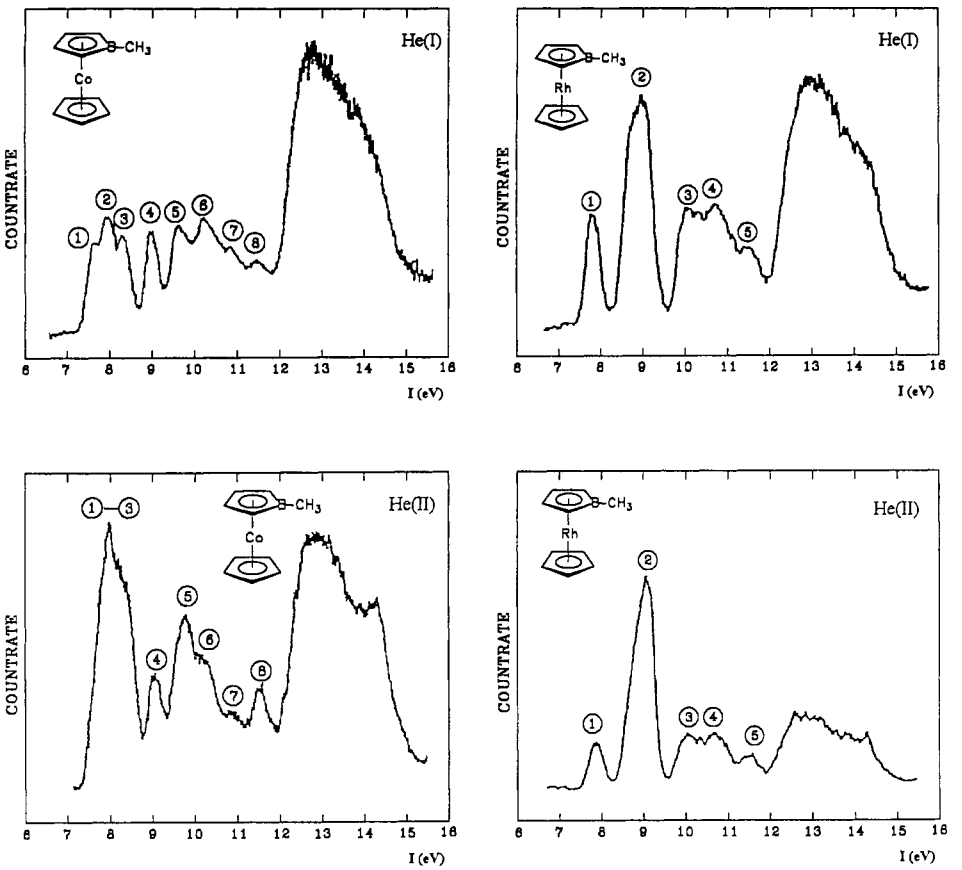


**Figure 4.** He I and He II photoelectron spectra of Cp–M–Bo (M = Co, Rh).

**Table 1. Relations of the Band Intensities (Expressed as Percentages) in the He I and He II Spectra of 1a and 2a**

| | $(C_4H_4BCH_3)Co(C_5H_5)$ (**1a**) | | | | | | $(C_4H_4BCH_3)Rh(C_5H_5)$ (**2a**) | | | | |
|---|---|---|---|---|---|---|---|---|---|---|---|
| | 1–3 | 4 | 5 | 6 | 7 | 8 | 1 | 2 | 3 | 4 | 5 |
| He I | 41 | 13 | 13 | 14 | 10 | 9 | 17 | 34 | 18 | 18 | 13 |
| He II | 55 | 9 | 13 | 10 | 6 | 7 | 11 | 54 | 14 | 14 | 7 |

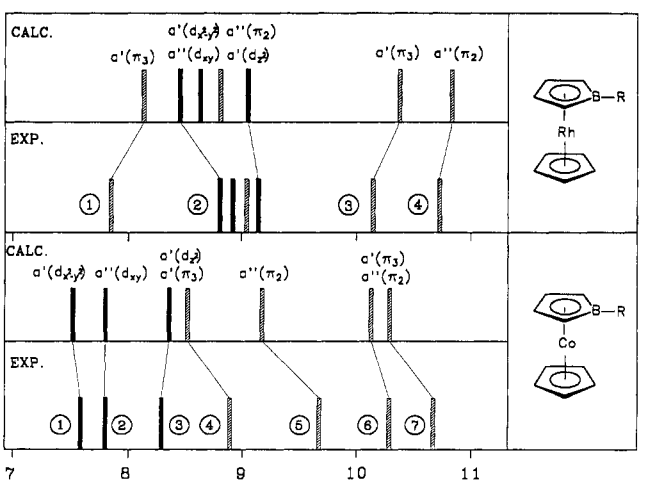


**Figure 5.** Assignment of the PE spectra of Cp–M–Bo (M = Co, Rh) based upon the ab initio CI calculations.

structure of the Cp and borole ligands. At lower energies, three distinct systems of bands are observed, centered at similar energies for both complexes, namely 7.7–7.9, 9.0, and 10.5 eV. This last system extends from 9.6 to 11.5 eV for **1a** and from 10.0 to 11.5 eV for **2a** and displays a similar structure composed of three peaks, with a shoulder at 10.9–11.0 eV more visible for **1a**. Even though the two first band systems appear at similar energies for **1a** and **2a**, their structures and relative intensities are noticeably different. In the cobalt system, the first band system is composed of three overlapping bands (bands 1–3), whereas complex **2a** displays a featureless peak at 7.7 eV, suggesting that it is associated with one ionization process. The same argument can be applied to band 4 of complex **1a**, a well-separated peak at 8.9 eV. The second peak of the rhodium complex, **2a**, is also featureless, but it is broad enough to suggest the contribution of several ionization events. The areas defined by the band envelopes are in the approximate ratio 3:1:5 for **1a** and 1:4:4 for **2a**. Those numbers can provide a guideline to estimate the number of ionization events associated with each band system. To assign the first bands in the PE spectra of **1a** and **2a** empirically, we compare the intensities of the He I and He II spectra, making use of the observation that the PE cross sections of ionizations from d orbitals and ligand MOs differ significantly.[22,23]

The comparison He I/He II for **1a** shows a pronounced increase of intensity for the first peak (bands 1–3) (see Table 1). In the case of **2a** the second peak (band 2) is increased considerably in the He II spectrum. These observations suggest the assignment of the first peak in the PE spectrum of **1a** (bands 1–3) to ionization processes

(23) Cauletti, C.; Green, J. C.; Kelly, M. R.; Powell, P.; van Tilborg, J.; Robbins, J.; Smart, J. *J. Electron Spectrosc. Relat. Phenom.* **1980**, *19*, 327.

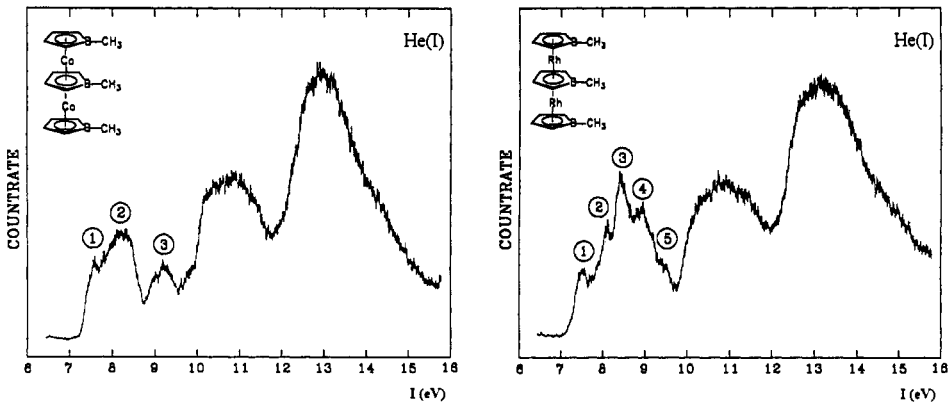


**Figure 6.** He I photoelectron spectra of Bo–M–Bo–M–Bo (M = Co, Rh).

**Table 2. Description of the Computed Vertical Ionization $I_{v,j}^{comp}$ at the ab Initio CI Level for 1b and 2b (All Energies in eV)**

| | | | | | | MO (NO) population analysis[e] | | | |
|---|---|---|---|---|---|---|---|---|---|
| MO[a] | $-\epsilon_j$[b] | relax[c] | $I_{v,j}^{comp}$ | $I_{v,j}^{exp}$ | band[d] | % M | % Bo | % Cp | fragment and metal orbital assgnt |
| | | | | | Cp–Co–Bo | | | | |
| 16a′ | 14.65 | +7.15 | 7.50 | 7.6 | 1 | 58 (92) | 18 (3) | 24 (5) | $x^2-y^2$ |
| 7a″ | 14.71 | +6.88 | 7.83 | 7.9 | 2 | 46 (91) | 32 (5) | 22 (4) | $xy$ |
| 15a′ | 16.52 | +8.50 | 8.42 | 8.3 | 3 | 58 (91) | 19 (4) | 23 (5) | $z^2$ |
| 18a′ | 8.30 | −0.24 | 8.54 | 8.9 | 4 | 23 (49) | 46 (41) | 31 (10) | $yz + \pi_3$: Bo, Cp |
| 10a″ | 9.29 | +0.12 | 9.17 | 9.6 | 5 | 17 (8) | 77 (49) | 6 (43) | $\pi_2$: Bo, Cp |
| 17a′ | 10.96 | +0.87 | 10.09 | 10.02 | 6 | 32 (29) | 18 (2) | 50 (69) | $yz + \pi_3$: Cp, Bo |
| 9a″ | 10.32 | +0.09 | 10.23 | | | 18 (55) | 5 (31) | 77 (14) | $xz + \pi_2$: Cp, Bo |
| | | | | | Cp–Rh–Bo | | | | |
| 18a′ | 7.84 | −0.21 | 8.05 | 7.7 | 1 | 15 (24) | 40 (38) | 45 (38) | $yz + \pi_3$: Bo, Cp |
| 16a′ | 12.14 | +3.78 | 8.36 | | | 64 (90) | 29 (4) | 7 (6) | $x^2-y^2$ |
| 11a″ | 11.76 | +3.19 | 8.57 | 9.0 | 2 | 67 (89) | 24 (6) | 9 (5) | $xy$ |
| 10a″ | 8.86 | +0.10 | 8.76 | | | 5 (7) | 47 (43) | 48 (50) | $\pi_2$: Bo, Cp |
| 17a′ | 11.76 | +2.73 | 9.03 | | | 87 (94) | 7 (4) | 6 (2) | $z^2$ |
| 15a′ | 11.04 | +0.68 | 10.36 | 10.1 | 3 | 42 (54) | 24 (6) | 34 (40) | $yz + \pi_3$: Cp, Bo |
| 8a″ | 11.08 | +0.31 | 10.77 | 10.7 | 4 | 42 (60) | 32 (16) | 26 (24) | $xz + \pi_2$: Bo, Cp |

[a] Labeling of the valence molecular orbital mainly involved in the ionization process. The labeling refers to Figure 1. [b] Koopmans' ionization energy. [c] Global influence of relaxation and correlation on the ionization energy. A plus sign means a decrease of the computed energy with respect to Koopmans' value. [d] The numbers refer to the band labeling of Figure 4. [e] Mulliken population analysis of the molecular orbital of the neutral molecule referred to in column 1 and (in parentheses) of the single occupied natural orbital obtained from the CI expansion.

originating from metal 3d orbitals and the second peak (band 4) to a ligand ionization process. For **2a**, however, the first band is assigned to an ionization event from a ligand orbital, whereas the second peak results from metal 4d orbitals.

The results of the ab initio CI calculations reported in Table 2 and in Figure 5 provide an interpretation of the photoelectron spectra of **1a** and **2a**. The key points for understanding the differences between the PE spectra of **1a** and **2a** are (i) the difference in the relaxation energies associated with the ionization of the $t_{2g}$-like metal orbitals of cobalt and rhodium and (ii) the larger crystal-field splittings expected for second-row ligated transition metals with respect to first-row metals in an equivalent environment.

The large relaxation energies obtained in relation with the ionization from metal orbitals in complexes of first-row transition metals are well documented within either the ab initio[13,22-24] or the semiempirical INDO treatment.[1,17] Those important relaxation effects are more specifically obtained with electron-rich metals, for which the 3d shell becomes extremely contracted and loses part of its valence-shell character. As a consequence, the withdrawal of an electron from an orbital with major cobalt 3d character will give rise to an ionized state displaying some similarities with a core hole state.[25,26] More specifically, quantum chemical calculations usually show that upon ionization of a metal 3d electron, the electron density flows from the surrounding ligands toward the metal in order to ensure a near constancy of the metal net charge in the ground state of the neutral molecule and in the ionized states. This reorganization of the electron density is at the origin of the relaxation energy, which has been shown from SCF calculations to modify Koopmans' value by more than 10 eV in bis($\pi$-allyl)nickel.[24] Correlation effects, which are also included in the present ab initio treatment, are generally going the opposite way because of the presence of one more electron pair to be correlated in the ground state of the neutral molecule. The same was also well documented for our Green's function approach with computational background of the INDO procedure.[17] It has been shown that the relaxation energy amounts to ca. 7 eV and that the ratio between relaxation and correlation corrections is 2:1 in the limit of strongly localized cobalt orbital 3d wave functions. The influence of relaxation remains largely dominant in metal-centered

(24) (a) Veillard, A.; Demuynck, J. In Modern Theoretical Chemistry; Schaefer, H. F., Ed.; Plenum Press, New York, 1977; Vol. 4, pp 187–222. (b) Hillier, I. H. *Pure Appl. Chem.* **1979**, *51*, 2183.

(25) (a) Cederbaum, L. S.; Domcke, W. *J. Chem. Phys.* **1977**, *66*, 5084. (b) Agren, A.; Bagus, P. S.; Roos, B. O. *Chem. Phys. Lett.* **1981**, *82*, 505. (c) Backsay, B. B.; Bryant, G.; Hush, N. H. *Int. J. Quantum Chem.* **1987**, *31*, 471. (d) Schwartz, W. H. E.; Chang, T. C.; Seeger, U.; Hwang, K. H. *Chem. Phys.* **1987**, *117*, 73.

(26) (a) Newton, M. D. *Chem. Phys. Lett.* **1982**, *90*, 291. (b) Messmer, R. P.; Caves, T. C.; Kao, C. M. *Chem. Phys. Lett.* **1982**, *90*, 296. (c) Benard, M. *Chem. Phys. Lett.* **1983**, *96*, 183.

**Table 3. Description of the Computed Vertical Ionization Energies $I_{v,j}$ at the INDO Level for 1a and 3a (All Energies in eV)**

| | | | | | | population analysis[f] | | | |
|---|---|---|---|---|---|---|---|---|---|
| MO[a] | $-\epsilon_j$[b] | relax[c] | $I_{v,j}^{comp}$[d] | $I_{v,j}^{exp}$ | band[e] | % Co | % Bo | % Cp | fragment and metal orbital assgnt |
| | | | | | Cp–Co–Bo | | | | |
| 7a″ | 12.42 | 4.82 | 7.60 | 7.60 | 1 | 86 | 10 | 4 | $xy$ |
| 16a′ | 11.97 | 3.86 | 8.11 | 7.90 | 2 | 66 | 16 | 18 | $x^2-y^2$ |
| 15a′ | 12.38 | 3.89 | 8.49 | 8.30 | 3 | 69 | 15 | 16 | $z^2$ |
| 18a′ | 9.11 | 0.43 | 8.68 | 8.90 | 4 | 15 | 41 | 44 | $yz+\pi_3$: Bo, Cp |
| *g* | 12.23 | 2.76 | 9.47 | | | 52 | 19 | 29 | $x^2-y^2, yz+\sigma$: Bo |
| 10a″ | 10.15 | 0.31 | 9.84 | 9.60 | 5 | 2 | 65 | 33 | $\pi_2$: Bo, Cp |
| 17a′ | 11.78 | 1.78 | 10.00 | 10.20 | 6 | 30 | 44 | 26 | $yz+\pi_3$: Bo, Cp |
| 9a″ | 11.00 | 0.85 | 10.15 | | | 13 | 55 | 32 | $xz+\pi_2$: Bo, Cp |
| 14a′ | 11.05 | 0.88 | 10.17 | | | 9 | 75 | 16 | $\sigma$: Bo, Cp |
| 11a″ | 11.52 | 1.10 | 10.42 | | | 24 | 55 | 21 | $xz, xy+\sigma$: Bo, Cp |
| | | | | | Bo–Co–Bo–Co–Bo | | | | |
| $14a_1$ | 12.07 | 4.66 | 7.41 | 7.5 | 1 | 90 | 10 | | $z^2$ |
| $10b_2$ | 12.40 | 4.61 | 7.79 | | | 89 | 11 | | $x^2-y^2$ |
| $7b_1$ | 12.51 | 4.46 | 8.08 | | | 83 | 17 | | $xy$ |
| $9b_2$ | 12.00 | 3.53 | 8.47 | 8.1 | 2 | 66 | 34 | | $z^2$ |
| $12b_2$ | 8.70 | 0.21 | 8.49 | | | 4 | 96 | | $\pi_3$: Bo |
| $4a_2$ | 12.45 | 3.67 | 8.78 | | | 66 | 34 | | $xy$ |
| $16a_1$ | 10.30 | 1.44 | 8.86 | 8.90 | sh | 38 | 62 | | $yz+\pi_3$: Bo |
| $15a_1$ | 12.16 | 3.14 | 9.02 | 9.10 | 3 | 62 | 38 | | $x^2-y^2$ |
| *g* | 12.14 | 2.91 | 9.23 | | | 54 | 46 | | $x^2-y^2, \sigma$: Bo |
| $11b_2$ | 10.40 | 1.07 | 9.33 | 9.60 | 4 | 22 | 78 | | $yz+\pi_3$: Bo |
| $10b_1$ | 11.37 | 1.66 | 9.71 | | | 22 | 78 | | $xy+\sigma$: Bo |
| $13a_1$ | 11.36 | 1.62 | 9.74 | | | 22 | 78 | | $z^2+\sigma$: Bo |
| $8b_1$ | 10.48 | 0.59 | 9.89 | | | 9 | 91 | | $\pi_2$: Bo |
| $6a_2$ | 10.51 | 0.59 | 9.92 | | | 8 | 92 | | $\pi_2$: Bo |
| $9b_1$ | 11.67 | 1.45 | 10.22 | | | 32 | 68 | | $xz, xy+\sigma$: Bo |
| $5a_2$ | 11.23 | 0.96 | 10.27 | | | 10 | 90 | | $\pi_2$: Bo |

[a] The labeling of the valence molecular orbitals refers to Figures 1–3. [b] Koopmans' ionization energy. [c] Global influence of relaxation and correlation on the ionization energy. [d] Computed ionization energy according to eq 2. [e] The numbers refer to the band labeling of Figures 1–3. [f] Mulliken population analysis of the molecular orbitals of the neutral molecule. [g] MO describing the B–$CH_3$ $\sigma$-bond; for discussion see text.

**Table 4. Description of the Computed Vertical Ionization Energies $I_{v,j}$ at the ab Initio CI Level for 3b and 4b (All Energies in eV)**

| | | | | | | MO (NO) population analysis | | | |
|---|---|---|---|---|---|---|---|---|---|
| MO[a] | $-\epsilon_j$ | relax | $I_{v,j}^{comp}$ | $I_{v,j}^{exp}$ | band[b] | % M | % $Bo_c$ | % $Bo_t$ | fragment and metal orbital assgnt |
| | | | | | Bo–Co–Bo–Co–Bo | | | | |
| $7b_1$ | 14.97 | +7.89 | 7.08 | 7.5 | 1 | 54 (98) | 15 (1) | 31 (1) | $xy$ |
| $4a_2$ | 15.05 | +7.45 | 7.60 | | | 66 (92) | 2 (2) | 32 (6) | $xy$ |
| $10b_2$ | 14.96 | +7.21 | 7.75 | | | 81 (97) | 3 (2) | 16 (1) | $x^2-y^2$ |
| $15a_1$ | 14.36 | +6.58 | 7.78 | 8.1 | 2 | 62 (95) | 14 (3) | 22 (2) | $x^2-y^2$ |
| $12b_2$ | 8.13 | –0.04 | 8.17 | | | 15 (20) | 40 (39) | 45 (41) | $xz+\pi_3$: $Bo_c$, $Bo_t$ |
| $14a_1$ | 16.32 | +8.09 | 8.23 | | | 73 (92) | 15 (6) | 12 (2) | $z^2$ |
| $16a_1$ | 9.39 | +0.99 | 8.40 | 8.9 | sh | 48 (60) | 10 (6) | 42 (34) | $yz+\pi_3$: $Bo_t$ |
| $9b_2$ | 17.34 | +8.92 | 8.42 | 9.1 | 3 | 63 (96) | 16 (0) | 21 (4) | $z^2$ |
| $11b_2$ | 11.19 | +1.43 | 9.76 | 9.6 | 4 | 48 (67) | 24 (22) | 28 (11) | $xz+\pi_3$: $Bo_c$, $Bo_t$ |
| $8b_1$ | 9.64 | –0.44 | 10.08 | | | 20 (31) | 3 (2) | 77 (67) | $xz+\pi_2$: $Bo_t$ |
| $6a_2$ | 9.73 | –0.45 | 10.18 | | | 18 (15) | 4 (13) | 78 (72) | $xz+\pi_2$: $Bo_t$ |
| $5a_2$ | 11.64 | +0.16 | 11.48 | | | 23 (46) | 64 (47) | 13 (7) | $xz+\pi_2$: $Bo_c$ |
| | | | | | Bo–Rh–Bo–Rh–Bo | | | | |
| $12b_2$ | 7.06 | +0.13 | 6.39 | 7.5 | 1 | 4 (6) | 51 (53) | 45 (41) | $\pi_3$: $Bo_c$, $Bo_t$ |
| $10b_1$ | 11.32 | +3.30 | 7.94 | 8.1 | 2 | 72 (92) | 17 (4) | 11 (4) | $xy$ |
| $16a_1$ | 11.46 | +3.38 | 8.08 | | | 79 (96) | 10 (2) | 11 (2) | $x^2-y^2$ |
| $15a_1$ | 9.52 | +1.08 | 8.44 | 8.5 | 3 | 51 (67) | 9 (3) | 40 (30) | $yz+\pi_3$: $Bo_t$ |
| $5a_2$ | 12.06 | +3.43 | 8.63 | | | 54 (91) | 4 (5) | 42 (5) | $xy$ |
| $11b_2$ | 12.01 | +3.34 | 8.67 | | | 83 (97) | 12 (2) | 5 (1) | $x^2-y^2$ |
| $7a_2$ | 9.32 | +0.64 | 8.68 | 8.8 | 4 | 4 (5) | 35 (38) | 61 (57) | $\pi_2$: $Bo_c$, $Bo_t$ |
| $14a_1$ | 12.03 | +3.12 | 8.91 | | | 70 (81) | 13 (11) | 17 (8) | $z^2$ |
| $10b_2$ | 12.63 | +2.72 | 9.91 | 9.5 | 5 | 67 (94) | 9 (4) | 24 (2) | $z^2$ |
| $9b_2$ | 11.44 | +1.21 | 10.23 | 9.8 | | 47 (80) | 18 (10) | 35 (10) | $yz+\pi_3$: $Bo_c$, $Bo_t$ |
| $7b_1$ | 10.37 | –0.01 | 10.38 | | | 30 (51) | 5 (2) | 65 (47) | $xz+\pi_2$: $Bo_t$ |
| $4a_2$ | 12.57 | +0.95 | 11.62 | | | 52 | 29 | 19 | $xz+\pi_2$: $Bo_t$, $Bo_c$ |

[a] The labeling of the valence MOs refers to that of Figures 2 and 3. [b] Refers to the band labeling of Figure 6.

ionizations: for the sandwich cobalt complex the overall effect of relaxation and correlation leads for the ionization of the $t_{2g}$-like cobalt orbitals to an energy decrease of 7.15–8.50 eV (ab initio CI) or of 3.89–4.82 eV (INDO) with respect to Koopmans' values (Tables 2 and 3). For ionizations originating in orbitals with a major weight on the ligand, the effects of relaxation and correlation are rather balanced,[17,22] and the difference with respect to Koopmans' energies never exceeds 1 eV (ab initio CI) or 1.80 eV (INDO) (Tables 2 and 3). Because of the overwhelming influence of relaxation, the three ionizations associated with the $t_{2g}$-like cobalt orbitals appear first in the calculations and should be correlated with the three peaks of the first band system at 7.60, 7.90, and 8.30 eV.

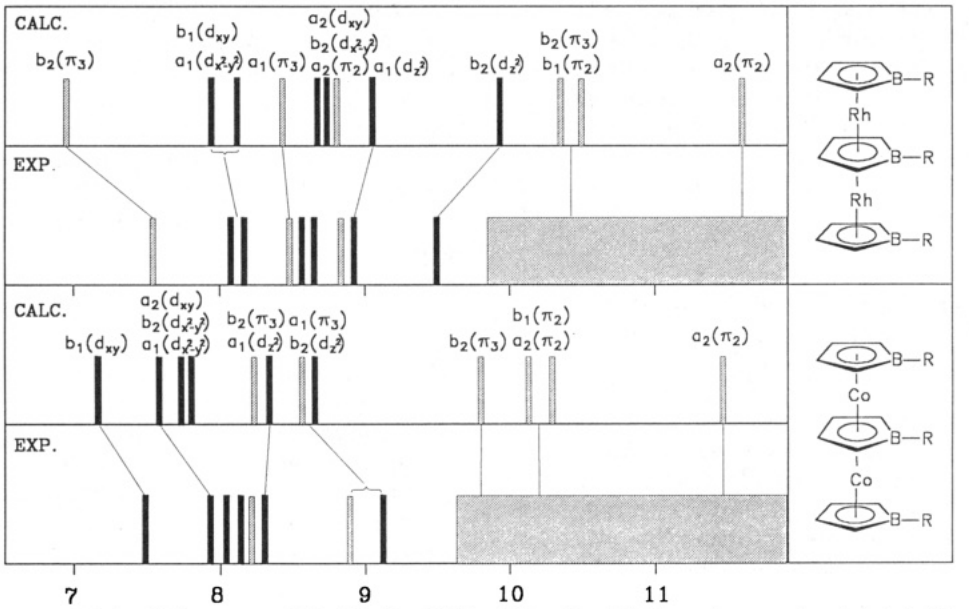


**Figure 7.** Assignment of the PE spectra of Bo–M–Bo–M–Bo (M = Co, Rh) based upon the ab initio CI calculations.

This assignment is in complete agreement with the relative enhancement of band system 1–3 obtained from He II spectroscopy. The second peak should be assigned to an ionization originating in the HOMO 18a′ of the EHT calculation.

According to the orbital diagram of Figure 1, the HOMO is the slightly destabilized term of an interaction between the $d_{yz}$ metal orbital and the frontier $\pi$-orbitals of both ligands. The ab initio CI calculations carried out on the ground state of the neutral molecule show that this orbital is associated with important, nondynamic correlation effects, eventually leading to an *increase* of the ionization energy with respect to Koopmans' value (Table 2).

The ionizations arising from the three remaining frontier orbitals with metal and $\pi$-ligand character, namely 9a″, 17a′, and 10a″ are computed to occur at 9.17 (9.84), 10.09 (10.00), and 10.23 (10.15) eV, respectively. The numbers in parentheses refer to INDO calculations. They should give rise to the first two peaks of the large band system starting at 9.6 eV. One should notice that ionizations arising from ligand orbitals with $\sigma$ character and more specifically from the relatively high-lying HOMO of the $[CoBo]^+$ subsystem (Figure 1) might also contribute to this band system. Those $\sigma$ states have not been included among the reference states of the CI calculations and therefore do not show up in the computed ab initio results. However, two of those states were considered in the INDO calculations. The computed ionization energies are 10.17 (14a′) and 10.42 (11a″) eV (Table 3). We remind that in the case of **1a** empirical assignment predicts five ionizations for the large band system starting at 9.6 eV. In this region the INDO calculations predict additionally one ionization ("a sixth contribution") from a relatively low-lying MO ($\epsilon_i$ = −12.23 eV) describing the B–$CH_3$ $\sigma$-bond (see Table 3). We believe that the calculated ionization energy of 9.47 eV is too low due to an "overestimated" Koopmans' defect as a result of a symmetry allowed large metal admixture (52%) to this MO, and it seems reasonable that this ionization should appear at a higher energy. A similar situation can occur in any case where the ground state wave function describes ligand levels not sufficiently separated in energy from metal levels and the mixing is symmetry allowed.[19a]

Let us now consider system **2**, the sandwich complex of rhodium. The 4d shell of the second-row transition metals is much more diffuse and valencelike than the 3d shell of the first-row metal with the same electronic configuration. Consequently, the reorganization of the electron density accompanying an ionization from a metal 4d orbital will remain moderate, as for the associated relaxation energy. The overall effect of relaxation and correlation for the $t_{2g}$-like metal orbitals of **2b** has led to an energy decrease of 2.7–3.8 eV only with respect to Koopmans' values. Eventually, the ionization energies originating in rhodium orbitals are computed to be 8.36, 8.57, and 9.03 eV, that is 0.6–0.8 eV *higher* than the corresponding ionization energies originating in the cobalt levels of **1b**. Because of this upward shift, the three rhodium d ionizations should be assigned to the *second* band of Figure 4. It seems however that band system 2 is not of pure metal origin, because of the insertion of one ionized state with mainly ligand character, calculated at 8.76 eV (Table 2). This ionization state should be related to orbital 10a″ of Figure 1. What is the origin of the single peak of band 1, observed at 7.7 eV? To understand it, one should refer to the larger crystal-field splittings observed in complexes of second- or third-row transition metals with respect to equivalent complexes of first-row metals.[27] This larger splitting is also a consequence of the more diffuse and valencelike character of the d metal orbitals, giving rise to a more efficient overlap and to enhanced interactions with the ligand orbitals. This point has already been discussed above in connection with the orbital interaction diagrams of Figures 1 and 2. The consequence is a broader scattering of the four energy levels issued from the interaction between the metal d and the ligand $\pi$-orbitals. This scattering is quantified as the computed energy difference between the highest and the lowest ionized states with main ligand character and amounts to 2.7 eV in **2b**, compared to 1.69 eV in **1b** (Table 2). More specifically, the HOMO 18a′ has risen in energy and the corresponding ionized state is calculated at 8.05 eV compared to 8.54 eV

(27) (a) Figgis, B. N. *Introduction to Ligand Fields*; Wiley-Interscience: New York, 1966. (b) Cotton, F. A.; Wilkinson, G. *Advanced Inorganic Chemistry*, 4th ed.; Wiley-Interscience: New York, 1980. (c) Griewe, G. L.; Hall, M. B. *Organometallics* **1988**, *7*, 1923.

in **1b**. This ionization at 8.05 eV should be assigned to the first band of the PE spectrum. To summarize, the ionized states with an unpaired electron localized on the metal appear at a *higher* energy, whereas the ionization associated with the ligand-based HOMO is shifted to *lower* energies. The consequence is an interchange between band systems 1–3 and 4 when going from cobalt to rhodium. This statement is in full agreement with the band intensities in He I and He II photoelectron spectra of **1a** and **2a** (Figure 1, Table 1).

A similar interpretation had been proposed by Green et al. to assign the PE spectra of cobalt, rhodium, and iridium cyclopentadienyl diene complexes.[28] It had been inferred from He I and He II PE spectra, and from qualitative MO schemes that "in the cobalt case, the HOMO is largely d in character, whereas for Rh and Ir, substantial localization on the ligands is indicated".[28] To our knowledge, this interchange between the two first band systems of sandwich complexes of Co and Rh had never been substantiated up to now from detailed calculations.

**IV.2. Triple-Decker Borole Complexes.** The He I photoelectron spectra of Bo–Co–Bo–Co–Bo (**3a**) and Bo–Rh–Bo–Rh–Bo (**4a**) are displayed in Figure 6. On the low energy side of the PE spectrum (7–9.6 eV), **3a** displays two band systems. The first band system is composed of two peaks at 7.5 and 8.1 eV. The second band system has one peak at 9.1 eV (peak 3) and a shoulder at 8.9 eV. The ratio of the areas below the envelopes of the two band systems is approximately 6:2, suggesting equal numbers of contributing ionizations (Figure 6). In the same region of the PE spectrum, complex **4a** has five overlapping bands with maxima at 7.5, 8.1, 8.5, 8.8, and 9.5 eV (Figure 6). Beyond 9.6 eV for **3a** and 9.8 eV for **4a**, a broad, featureless band is observed in both PE spectra. Then comes, beyond 12 eV, the intense band characteristic of the hydrocarbon framework.

The reference space of the ab initio CI calculation carried out on **3b** and **4b** has been designed to account for the 12 doublet states issued from the ionization of the six $t_{2g}$-like metal levels on the one hand (Figure 3) and of the six highest occupied levels with important $\pi$-ligand character resulting from interactions with d metal orbital combinations (Figure 2) on the other hand.

As conspicuously as for the sandwich complexes **1b** and **2b** the calculations provide evidence for an interchange in the assignment of the two first bands of the borole triple-decker complexes of cobalt and rhodium (Table 4, Figure 7). This interchange still can be explained by the double effect of the valence d shell expansion in the rhodium complex: (i) a considerable reduction of the relaxation energy associated with the ionization of the $t_{2g}$-like metal orbitals and (ii) an increased metal–ligand overlap pushing toward high energies the HOMO $12b_2$, delocalized over the $\pi$ systems of the three borole ligands.

In the cobalt complex **3** the global effect of relaxation and correlation is between 6.58 and 8.92 eV (ab initio CI) or between 3.14 and 4.66 (INDO). Band 1 and most contributions to band 2 (four out of five) should therefore be assigned to ionizations arising from metal levels. The ionized state associated with the HOMO ($12b_2$) shows up at 8.17 eV (ab initio CI) or 8.86 eV (INDO) and takes place as the fifth contribution to band 2, and the only one with major ligand character. Both calculation methods yield no clear energy separation between the five contributions to be assigned to band 2 and the two next ionized states, so that the assignment we propose for band 3 is no more than tentative. We suggest that band 3 should be assigned to two ionization events computed at 8.40 and 8.42 eV (ab initio CI) or 8.86 and 9.02 eV (INDO). One is associated with the second occupied MO ($16a_1$) which is largely delocalized over both the metal atoms and the ligand $\pi$ systems. The second involves the $t_{2g}$-like metal orbital. In the ab initio CI treatment this orbital is the out-of-phase combination of $d_{z^2}$ orbitals suited for a stabilizing interaction with the lowest $\pi$-orbitals of the three borole rings. In spite of a large relaxation effect, close to 9 eV, this doublet state remains high in energy, at 8.42 eV above the ground state of the neutral molecule. In the INDO treatment ionization from the $9b_2$ orbital contributes to band 2 and the second ionization in band 3 involves a linear combination of cobalt $x^2 - y^2$ orbitals. This discrepancy can be traced back to the slightly different mixing of the metal centered orbitals with the ligand $\pi$ and $\sigma$ systems in the ab initio and INDO ground state wave function of the neutral molecule. The four remaining doublet states considered in the ab initio CI treatment are computed to appear between 9.76 and 11.48 eV. They are assigned to the broad band system observed beyond 9.60 eV. Ionizations arising from the $\sigma$-orbitals of the borole ligands, such as $10b_1$ (Figure 2) are also expected to contribute to this band system, and INDO results (Table 3) confirm this hypothesis.

Peaks 1 and 2 of the Bo–Rh–Bo–Rh–Bo (**4a**) are observed at exactly the same energy as for the equivalent complex of cobalt, that is 7.5 and 8.1 eV, respectively. However, the calculations reported in Table 4 unambiguously show that those two bands have been interchanged. In the rhodium complex, the two first ionizations with major metal character (combinations of $d_{xy}$ and $d_{x^2-y^2}$ orbitals, respectively) are computed at 7.94 and 8.08 eV and should be assigned to band 2. On the other hand, the ligand-based HOMO has been pushed up in energy because of the enhanced interactions with rhodium d orbitals. The lowest ionization arising from the ligand $\pi$ system is then computed at 6.93 eV, that is 1.34 eV less than that for the equivalent state of the cobalt complex (8.17 eV). This $^2B_2$ state should be assigned to the first peak in the PE spectrum of **4a** (Figure 6).

The two next peaks, 3 and 4, of the observed spectrum have been jointly assigned to a batch of five ionized states computed between 8.44 and 8.91 eV. Three of those ionizations arise from pure metal levels. The two other ones, at 8.44 and 8.68 eV, respectively, are associated with the delocalized orbitals $15a_1$ and $7a_2$. As for the cobalt complex, the out-of-phase combination of the $d_{z^2}$ metal orbitals is very deep in energy and the corresponding ionized state is found to be well separated in energy from the other doublet states with d metal origin. The computed IP is 9.91 eV and the corresponding state is assigned to band 5.

More generally, the calculation yields for all four considered molecules an unexpectedly large scattering of the energies of the doublet states with major metal character: 1 eV for **1b** and **2b** and 1.34 and 1.37 eV for **3b** and **4b**, respectively (Tables 2 and 4).

(28) (a) Green, J. C.; Powell, P.; van Tilborg, J. E. *Organometallics* **1984**, *3*, 211. (b) Frankcom, T. M.; Green, J. C.; Nagy, A.; Kakkar, A. K.; Marder, T. B. *Organometallics* **1993**, *12*, 3688.

## V. Conclusion

He I photoelectron spectra of sandwich complexes of cobalt and rhodium with 18 and 30 electrons involving borole ligands have been reported and assigned on the basis of ab initio CI and INDO calculations, accounting for relaxation and correlation effects. Both calculations provide a delocalized description of the ionic states. They lead to a similar description of the photoelectron spectra of cobalt complexes. On the basis of ab initio CI calculations, it was shown that the replacement of cobalt by rhodium leads to an interchange of the first two band systems. This interpretation is supported by the He II spectra of **1a** and **2a**. The $t_{2g}$-like levels of cobalt are subject to large relaxation effects due to the contracted character of the 3d shell.

## Experimental Section

The preparation of compounds **1–4** has been described in the literature.[3,4] The He I photoelectron spectra of **1–4** have been recorded with a PS 18 instrument from Perkin-Elmer (Beaconsfield, England). The He II PE spectra of **1** and **2** have been recorded on an instrument from Helectros Developments (Beaconsfield, England). The recording temperatures were as follows: (**1**) 33 °C (He I), 42 °C (He II); (**2**) 48 °C (He I), 60 °C (He II); (**3**) 105 °C (He I); (**4**) 124 °C (He I). The calibration was done with Ar (15.76 and 15.94 eV) and Xe (12.13 and 13.44 eV). A resolution of 0.20 meV on the $^3P_{3/2}$ Ar line was obtained.

**Acknowledgment.** The calculations have been carried out on the CRAY-2 computer of the Centre de Calcul Vectoriel de la Recherche (Palaiseau, France), with computer time allocation from the CNRS (ab initio) and on the IBM-3080 computer of the Universitätsrechenzentrum Heidelberg (INDO). We are grateful to the Deutsche Forschungsgemeinschaft (SFB 247) and the Fonds der Chemischen Industrie for financial support. We thank A. Flatow for recording the He I PE spectra and the Helectros Developments for recording the He II PE spectra.

OM930412Z